

# EXPANSION ANGLE'S IMPACT ON THE LIFT TO DRAG RATIO OF THE CONE- DERIVED WAVE RIDER

Zhen-qing Wang\*, Cui-e Zhang\*, Kou-an Hao\* and Hong-qing Lv\*

## ABSTRACT

The waverider configuration is considered as the ideal aerodynamic configuration for hypersonic flight vehicle. Isentropic expansion design is done to the upper surface, and higher lift to drag ratio is obtained. Expansion angle is used as one of the variables when optimization is done by complex method. Higher lift to drag ratio can be obtained without penalty of useful volume. In addition, the balance of lift and weight must be considered when a flight vehicle is designed, especially for a cruise flight.

**Key words:** cone-derived waverider; expansion angle; lift to drag ratio; complex method

## 1. INTRODUCTION

Compared with generic vehicle configurations, the predominant advantage of waverider configuration is higher lift to drag ratio (L/D) obtained. When flying in its design state (i.e. supersonic or hypersonic), a promising candidate to break down the “lift to drag barrier” of Kuchemann is the waverider configuration[1][2][3]. The entire bow shock is attached to the leading edge of the body, so there is no flow spillage from the lower surface to the upper surface accordingly. As a result, the high pressure behind the shock wave leads to a considerably higher L/D than that for a generic shape. Because the vehicle appears to be riding on top of the attached shock wave when flying at its design point, hence it is dubbed the “waverider”.

In 1959, for the first time, Nonweiler designed the waverider with a caret-shaped cross-section, like “Λ”, and a delta platform. Scientists and engineers have been attracted to do considerable researches on constitution methods, integrated design and optimization on waverider configuration. It is found that the waverider is quite suitable for a hypersonic lifting body. However, the L/D is discovered to be lower in experiments and applications than in theoretical calculation [4]. It turns out that the influence of viscous should be emphasized during calculation, on the other hand, the L/D is attempted to further enhance by improvements in design. To realize the latter one, expansion design could be carried out on the upper surface. In the 5th literature, the angle of attack was taken as the expansion angle of the upper surface, when the maximum L/D was obtained, which increased the L/D by 37%. But the volume was reduced by folding down the upper surface directly, especially the height of volume.

In this paper, expansion angle is used as one of the variables when optimization is done. Not only higher L/D is obtained, but also the size of useful volume is guaranteed. In addition, it is found that if the balance of lift and weight considered, the L/D will decrease greatly. This might partly explain the reason why the L/D is discovered to be lower in applications than in theoretical calculation.

## 2. OPTIMAL DESIGN FOR WAVERIDER CONFIGURATION

Two conditions are required for the constitution of waverider configuration. First is the source flow field, and second is the baseline for design, generally the leading edge curve.

---

\* College of Aerospace and Civil Engineering, Harbin Engineering University, Harbin 150001, China, E-mail: wangzhenqing@hrbeu.edu.cn

## 2.1. Source Flow Field

The source flow is formed as the supersonic flow field moving through the cone flow field, at zero angle of attack. Taylor-Maccoll flow equation [6] is calculated by four-order Runge-Kutta numerical solution. The control equation of flow field and conditions for irrotational flow are shown as follows:

$$(\bar{v} \cdot \bar{\nabla}) \left[ \frac{v^2}{2} \right] - a^2 \bar{\nabla} \cdot \bar{v} = 0 \quad (1)$$

$$\bar{\omega} = \bar{\nabla} \times \bar{v} = 0 \quad (2)$$

After the determination of 3-D flow field, the lower surface is obtained through the streamline along the leading edge curve according to the flow equation. The streamline equation, in Cartesian space, can be expressed as:

$$\frac{dx}{v_x} = \frac{dy}{v_y} = \frac{dz}{v_z} \quad (3)$$

The leading edge of the upper surface parallels to the flow. After a certain distance, isentropic expansion design is done.

## 2.2. Parametric Design Methods

To facilitate the optimum design, parametric design is adopted, which is shown in figure 1. The surface of Cone-derived waverider could be determined by Mach, shock angle and the leading edge curve. While the leading edge curve, on the cone surface of shock wave, which is a space curve, is inconvenience for definition. As a result, the projection of the leading edge curve on the cone bottom is chosen as the original definition during design. The projection line is defined by four number of times function:

$$y = -az^4 + bz^2 + c \quad (4)$$

Where a, b and c are undetermined coefficients. The length of the waverider is given,  $L_d = 60$ . The intersection where the projection line and shock cone bottom intersect, is just the one where the leading edge and shock cone bottom intersect. The angle, between the connection from the point to the centre of bottom, and the symmetric plane, is dubbed the semi-unfold angle. The semi-unfold angle reflects the percentage of conical flow field in the cone flow field. What's more, the bigger the semi-unfold angle is, the more obvious the characteristic of cone flow will be, on the contrary, the more obvious the characteristic of flat-panel flow will be.

## 2.3. Aerodynamics Calculation

To realize rapid calculation for optimal design, the inviscid aerodynamic can be obtained by numerical the aerodynamic pressure integration on the plane, and the inflow static is considered as bottom drag. The reference

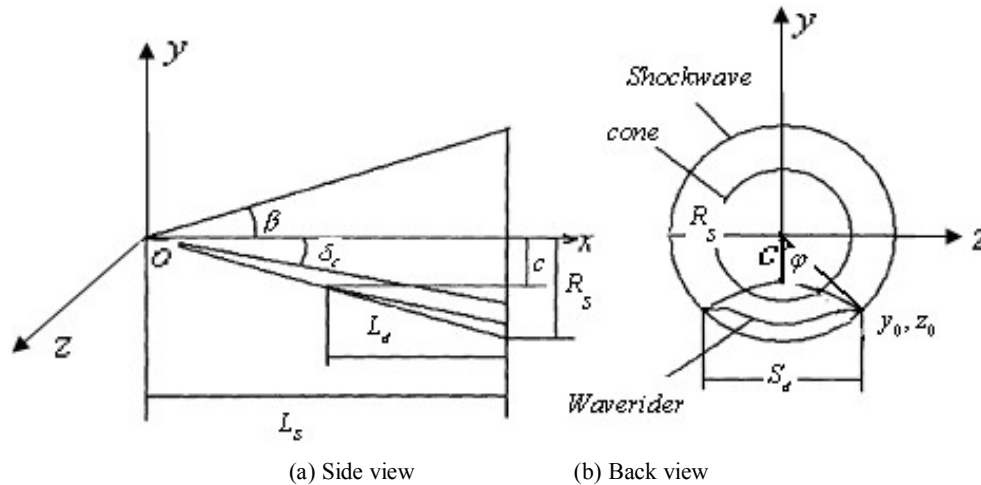


Figure 1: Schematic Diagram for Waverider Configuration

temperature method of Young and Janssen[7] is adopted to calculate the viscous force on the surface. For turbulence, the viscous stress equation is:

$$\tau = \frac{0.0592}{\text{Re}_x^{*0.2}} \frac{1}{2} \rho^* V_e^2 \quad (5)$$

Which,

$$\rho^* = \frac{P_e}{RT^*} \quad (6)$$

$$\text{Re}_x^* = \frac{\rho^* V_e x}{\mu^*} \quad (7)$$

Where,  $V_e$  is the flow velocity adjacent to boundary layer, adopting the velocity in inviscid flow during the calculation;  $x$  is the length from the leading edge, in the same direction of streamline;  $\mu^*$  is determined by the Sutherland's law, which is expressed in the international system of units as:

$$\mu^* = \mu_{ref} \left( \frac{T^*}{T_{ref}} \right)^{1.5} \frac{T_{ref} + S}{T^* + S} \quad (8)$$

When the reference temperature  $T_{ref} = 288\text{K}$ , the inviscid coefficient of the reference force  $\mu_{ref} = 1.789 \times 10^{-5} \text{ kg/m sec}$ ;  $S$ , the characteristic temperature of gas, for atmosphere is  $110\text{K}$ .

Reference temperature  $T^*$  is determined as follows:

$$\frac{T^*}{T_e} = 1 + 0.032 M_e^2 + 0.58 \left( \frac{T_w}{T_e} - 1 \right) \quad (9)$$

Which,  $T_w$  is the wall temperature. When Mach is 6, it is  $1100\text{K}$ . The calculation formula for viscous stress of laminar flow is:

$$\tau = \frac{0.664}{\sqrt{\text{Re}_x}} \frac{1}{2} \rho^* V_e^2 \quad (10)$$

The condition is determined by Bowcutt and Anderson's data:

$$\log \text{Re}_x = 6.421 e^{1.209 \times 10^{-4} M_e^{2.641}} \quad (11)$$

where,  $\text{Re}_x$  is Reynolds number based on the local distance  $x$ ,  $M_e$  is the Mach at the outer edge of local boundary layer.

### 3. OPTIMIZATION METHOD

After the basic flow field is determined, the leading edge curve is the deciding factor for the aerodynamic. The optimization is realized by the complex method through changing the shape of leading edge curve [8]. Complex method is an important direct algorithm for solving constrained optimization problems. The basic idea is that the initial complex, which the vertices number is  $k$ , is constructed in feasible region. Compare the objective function of each vertex on the initial complex, and find the vertex with the maximum function value (called the worst point), and find possible new point whose function value decreases by ways of reflection, expansion, contraction, narrow edge, then with the new one as the worst one, and constitute a new complex. Each time the complex shape changes, on the merits of moving toward the optimization, until approaching the optimal point mostly.

The optimal variables are the shock angle  $\beta$ , the semi-unfold angle  $\phi$ , the length to width ratio  $\sigma$ , the coefficient  $b$ , the expansion angle  $\alpha$  and so on. Maximum  $L/D$  as the objective function  $b$ , the height of the volume space, between the two thirds of length and one third of span wise length is larger than  $4\text{m}$ . The waverider configuration is optimized due to the five variables all above. The design Mach is  $6.0$ , altitude is  $30\text{km}$ .

#### 4. PROCEDURE AUTHENTICATION

The procedure, on constitution of cone-driver waverider configuration and the function calculation on design point, is written based on the preceding theory. The result for cone-derive waverider configuration added viscous optimization, at Mach 6, altitude 30km, is given in the 9th literature. The result is generated by MAXWARP procedure. According to the leading edge curvilinear coordinates given by the literature, the cone-derive waverider configuration is generated as well as the function calculation on the design point. The table 1 shows the coincidence between the two. MAXWARP is the benchmark for waverider configuration design. The result, in this paper, is basically consistent with proceeding, which proves the effectiveness of the procedure, and it can be used to generate the configuration for cone-derive waveride as well as the function calculation.

**Table 1**  
Contrast with the Function Parameters

	$C_L$	$C_D$	$L/D$	$V(m^3)$	$V_{eff}$
MAXWARP	3.168E-2	4.089E-3	7.74	2327	5.998E-2
Procedure	3.152E-2	4.073E-3	7.74	2329	6.17E-2
Error (%)	-0.51	-0.39	0	0.086	2.87

Note:  $V$  for the waverider configuration of the volume,  $V_{eff}$  for the volumetric efficiency.

#### 5. RESULT ANALYSIS

First of all, determine the upper and lower limits for each variable through the analysis on the function parameters. In order not to bring forth large deformation to waverider configuration for expansion angle, the upper limit of expansion angle is set at  $5^\circ$ .

##### 5.1. Determination of Distance

The expansion angle helps to make sharper leading edge, which will not only exacerbate the difficulty for thermal protection there, but also aggravate the stress concentration for configuration. In this paper, it is envisaged that the expansion is designed a certain distance away from the leading edge, while the distance is recorded as  $L_p$ . The impact on  $L/D$  is shown in figure 2. The abscissa is dimensionless by the length of waverider configuration, while the ordinate is dimensionless by the  $L/D$  value as  $L_p = 0$ . It can be seen that the  $L_p$  has little impact on  $L/D$ , and the maximum  $L/D$  is obtained when  $L_p = 1\%$ .  $L_d$  in this paper.

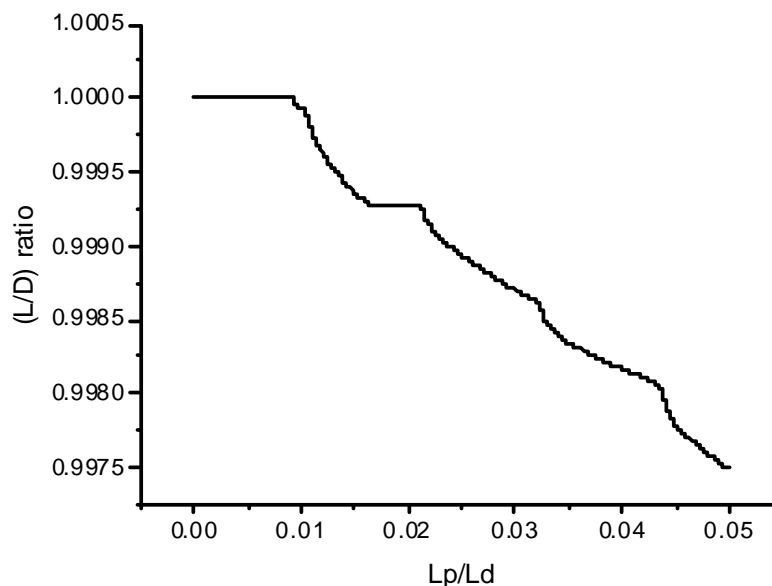


**Figure 2:** Schematic of  $L/D$  with  $L_p$

## 4.2. Optimization Results

Bond in the same conditions, the waverider configuration is optimized in two conditions whether the expansion angle is zero or not. The results are shown in table 2, and the design parameters corresponding to optimal solution are shown in table 3. In table 2,  $V_E$  is useful volume of which the height is larger than 100mm. After expansion design done to the upper surface, not only the L/D increases by 8.15%, but also the volumetric efficiency and useful volume increase by 8% and 11.5%.

**Table 2**  
Comparison Expansion with Non-expansion

	$L/D$	$V_{eff}$	$V_E(m^3)$	$D(T)$	$W(T)$	$L(T)$
Non-expansion [1]	8.711	0.051	3494	10.23	217.3	89.11
expansion [2]	9.421	0.054	3896	12.79	242.3	120.5
Error (%)	8.15	8	11.5	25	11.5	35.2

**Table 3**  
Parameters Corresponding to Optimal Solution

	$\psi(^{\circ})$	$b$	$\sigma$	$\beta(^{\circ})$	$\alpha(^{\circ})$
Non-expansion [1]	44.2	0.013	1.2	11.6	0
expansion [2]	16.4	0.0018	1.27	12.37	0.533

In contrast, the optimal configuration based on non-expansion angle, is optimized just for expansion angle again, with other constraints remaining. The results are shown in table 4. Under such circumstances, because of the height limit, the expansion angle only could be  $0.0003^{\circ}$ , and the L/D and volumetric efficiency are almost unchanged. This also shows that the optimization in this paper could obtain better results with constraints.

**Table 4**  
Comparison of the Function

	$L/D$	$V_{eff}$	$V_E(m^3)$	$D(T)$	$W(T)$	$L(T)$
Non-expansion	8.711	0.051	3494	10.23	217.3	89.1
expansion	8.714	0.051	3488	10.2	217.1	88.9
Error (%)	0.003	0	-0.17	-0.29	-0.009	-0.22

The 1st and 2nd results of optimization, the bottom contour map of waverider configuration, are given in the figure 3, 4. And L/D and drag coefficient, with the change of iterations, are given in figure 5, 6. In the iterative process, mainly the shape changes. And the shape has little impact on the viscous force. That is with the determination of the Mach and the design height, the viscous force has been little changed. In addition, the viscous force is about one third of the total drag from the figure 3, so its impact must not be ignored.

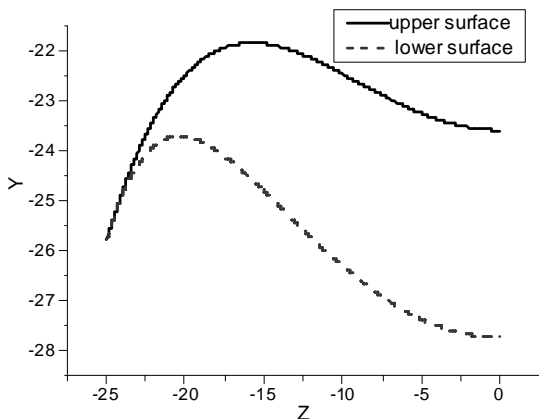


Figure 3: Bottom Contour Map at Zero Expansion Angle

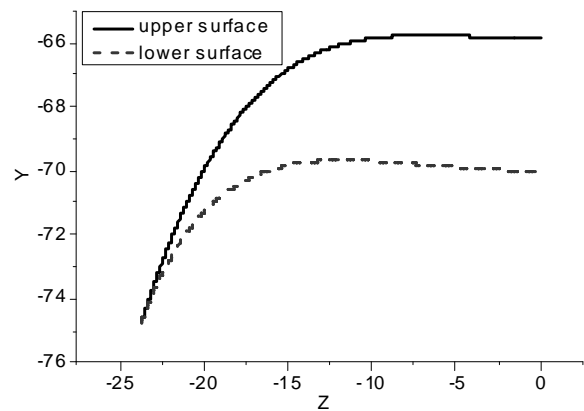


Figure 4: Bottom Contour Map at Certain Expansion Angle

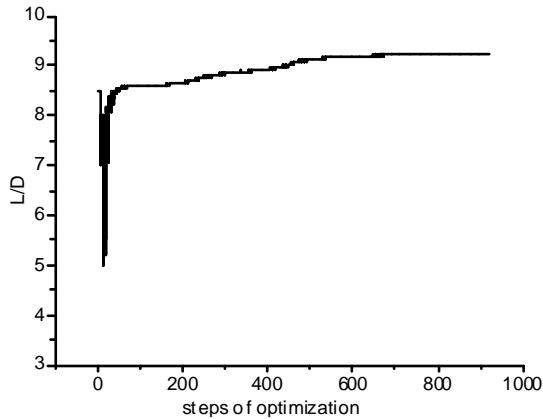


Figure 5: Schematic of L/D with the Iterations

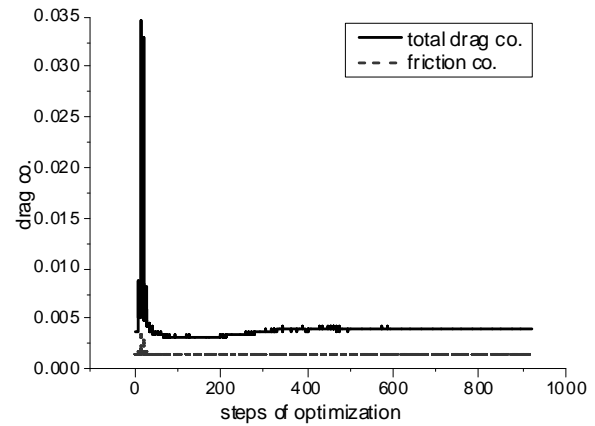


Figure 6: Schematic of Drag Coefficient with the Iterations

### 4.3. Optimization Results Considering Weight

Referring to the optimization result, the weight of the waverider configuration, without considering the balance of lift and weight, is far larger than the lift provided by it. The optimization result is unreasonable for flight vehicle in application, especially for a cruise flight. To make the waverider more practical, based on the above, the constraint, lift equal to weight, is added in this paper. The statistical result, given in the 10th literature, is used to estimate the weight. That is the average density is about  $124.2 \text{ kg} / \text{m}^3$  for entirely waverider configuration.

**Table 5**  
Comparison Expansion with Non-expansion

	$L/D$	$V_{eff}$	$V_E(m^3)$	$D(T)$	$W(T)$	$L(T)$
Non-expansion [3]	2.625	0.129	10227	229.9	635.1	603.5
expansion [4]	3.127	0.117	6279	119.3	390	372.9
Error (%)	19.1	-9.3	-38.6	-48.4	-38.6	-38.2

**Table 6**  
Parameters Corresponding to Optimal Solution

	$\psi(^{\circ})$	$b$	$\sigma$	$\beta(^{\circ})$	$\alpha(^{\circ})$
Non-expansion [3]	17.7	-0.14	1.48	27	0
expansion [4]	14.3	-0.21	2.23	24.2	1.83

After the balance of lift and weight considered, the L/D is only one third of the progenitor. In order to balance the lift and weight, the shock angle becomes twice bigger than expansion angle. After isentropic expansion design done to the upper surface, the shock angle decreased by  $2.8^{\circ}$ . As a result, the drag of waverider configuration is reduced greatly, despite the volumetric efficiency decreases by 9.3%. After optimization, all the function parameters are very satisfaction. The 3rd and 4th results of optimization, the bottom contour maps of waverider configuration, are given in the figure 7 and 8.

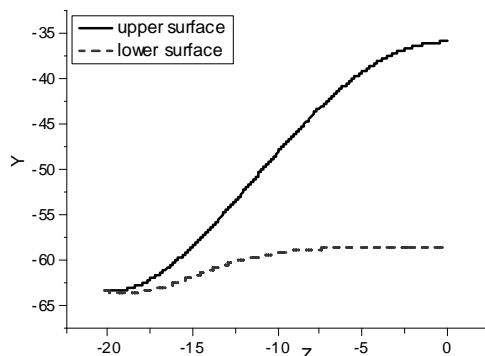


Figure 7: Bottom Contour Map at Zero Expansion Angle

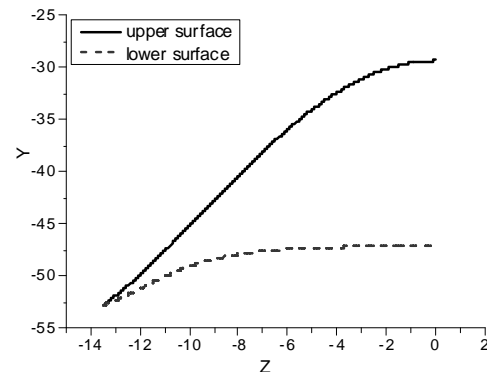


Figure 8: Bottom Contour Map at Certain Expansion Angle

## 5. CONCLUSION

Through optimization for the calculation in this paper, a few conclusions are obtained as follows:

- (1) Expansion angle is used as one of the variables when optimization is done by complex method. Higher L/D can be obtained without penalty of useful volume.
- (2) The impact of viscous force must be considered while designing waverider configuration.
- (3) When the balance of lift and weight considered, the L/D will be significantly reduced, which is only one third of the progenitor.
- (4) Without considering the weight, the shock angle is about  $12^\circ$  corresponding to the maximum L/D. While considering the weight, the shock angle is about  $27^\circ$ . After isentropic expansion design done to the upper surface, there will be slight change in angle shock.

### *Reference*

- [1] Bowcutt K. G., Anderson J. D. Jr, Capriotti D. Viscous Optimized Hypersonic Waveriders. AIAA 87-0272, 1987.
- [2] Corda S., Anderson J. D. Jr. Viscous Optimized Hypersonic Waveriders Designed from Axisymmetric Flow Fields. AIAA-88-0369, 1988.
- [3] Kuchemann D. The Aerodynamic Design of Aircraft. London, Pergamon Press, 1978.
- [4] ZHAO Gui-ling, HU Liang and WEN Jie. Research on Waverider Configuration and Aircraft. Mechanical Progress, 2003, 33(3): 357-374.
- [5] Wang Yankui, Zhang Dongjun, Deng Xueying. The Design of Waverider Configuration with High Lift-drag Ratio. 2005, AIAA 2005-6040.
- [6] Zucrow, Hoffman. Aerodynamics. National Defense Industry Press, 1989.
- [7] ZHANG Jie-qian, ZHANG Guang-hua and CHEN Yu-wen. Real hydromechanics. Beijing: University of Tsinghua, 1986.
- [8] SUN Jing-min. Optimal Design of Machinery. Beijing: Machinery Industry Press, 1999.
- [9] Naruhisa Takashima. Navier-stokes Computations of a Viscous Optimized Waverider. Master Thesis, University of Maryland, 1992, 06.
- [10] O'Neill. Optimized Scramjet Engine Integration on a Waverider Airframe. Doctor Thesis, University of Maryland, 1992.